WIRE-GRID SIMULATIONS OF THE MARS EXPRESS/MARSIS ANTENNA SYSTEM

W. Macher*, D. Plettemeier†, H.O. Rucker*, and G. Fischer*

Abstract

The MARSIS experiment (Mars Advanced Radar for Subsurface and Ionosphere Sounding) onboard Mars Express is a ground penetrating radar for the investigation of the Martian surface and subsurface structure. A particular objective is the search for underground water and ice, which is thought to be essential in the evolution of microbial life. The MARSIS antenna system consists of a primary dipole and a secondary monopole. The dipole transmits radar pulses and receives their echoes from the surface. The monopole is only used as a receiving antenna, serving for the cancellation of surface clutter echoes. An exact knowledge of the reception properties of the antenna system is essential for the evaluation of the sounding measurements. These properties, in particular the monopole gain and the effect of polarization, are perturbed by the spacecraft body. Numerical simulations are performed to determine the deviation from the idealized dipole and monopole behavior, respectively. The influences of the antenna feed configuration and various spacecraft parts are illustrated. Furthermore, the effect of the dipole matching network and the consequences of wave polarization are discussed.

1 Introduction

The primary scientific objective of MARSIS is the analysis of the subsurface layers of the Martian crust and the search for possible underground water reservoirs, detected as liquid-water- or ice-interfaces. For that purpose the MARSIS experiment uses a low-frequency nadir-looking radar sounder in the frequency range 0.1–5.5 MHz with ground penetrating capabilities, depending on the frequency of the transmitted pulse [Picardi et al., 2004]. Short pulses released from the dipole antenna travel to the Martian surface where they suffer a partial reflection. A small fraction of energy is transmitted into lower Martian surface layers, with additional potential reflections at subsurface dielectric discontinuities. This results into echoes with different time delays when arriving at the MARSIS antennas, depending on the depth of penetration and the wave propagation speed in the subsurface

* *Space Research Institute, Austrian Academy of Sciences, Schmiedlstrasse 6, A-8042 Graz, Austria*
† *Electrotechnical Institute, University of Dresden, Germany.*

medium. Off-nadir surface echoes (surface clutter) could evidently come back with the same time delays. Appropriate measurements have thus to be considered in order to separate the surface clutters from the subsurface echoes, thereby improving water/ice layer detection. Reduction of off-nadir surface clutter can essentially be obtained a) by applying Doppler azimuth processing on along-track returns, b) by subtracting off-nadir cross-track returns received by the nadir-pointing monopole antenna from the primary antenna return signal, and c) by comparison of echoes of different frequency bands [Picardi et al., 1999].

The present investigation focuses on the technique b) requiring an accurate knowledge of the MARSIS antenna reception properties, which are determined by computer simulations. The numerical analysis is performed in 3 steps:

1. the representation of the spacecraft (including all relevant parts mounted outside) and its antenna system as a suitable wire-grid model,
2. the calculation of the currents on the wire-grid for the transmission mode by means of an electromagnetic code, which numerically solves the underlying boundary value problem by the method of moments [Harrington, 1968], and
3. the determination of relevant parameters based on the currents calculated in step 2: antenna impedances, null-axes, gain, and polarization properties.

2 Spacecraft model and matching network

The Mars Express wire-grid model was built to get a realistic representation of the transmission and reception properties of the MARSIS antenna system. The following main features were thus implemented in the simulation: the central body, the high gain antenna, the thruster, the solar panels, the primary dipole (2 separate arms) and the secondary monopole (Figure 1). The Mars Express orbiter moves in the direction along the orientation of the solar panels, the dipole arms are cross-track oriented, and the monopole is along the nadir direction pointing away from the Martian surface. The right panel of Figure 1 shows a bent monopole. This is the bend used to simulate the effect of solar heating. The effect of this among several other configuration changes is studied as outlined below. The influence of the conductivity of the model wires on the results has been tested by running simulations with various conductivities. No appreciable influence of the conductivity (above 1 MS/m) has been found. Therefore the final calculations were made with the same conductivity of 50 MS/m (close to copper) for the whole model.

First studies revealed that the matching network, which is used for the two dipole elements to get a uniform power delivery over each frequency band, has a tremendous influence on the transmission and reception properties of both antennas [Macher et al., 2002]. Therefore all results presented here take into account the matching network. A block diagram of the network parts is shown in Figure 3. Each dipole element (arm) is connected to its own matching network. The passive elements between the antenna feeds and the networks, including the cables, are implemented as parts of the respective network circuit.

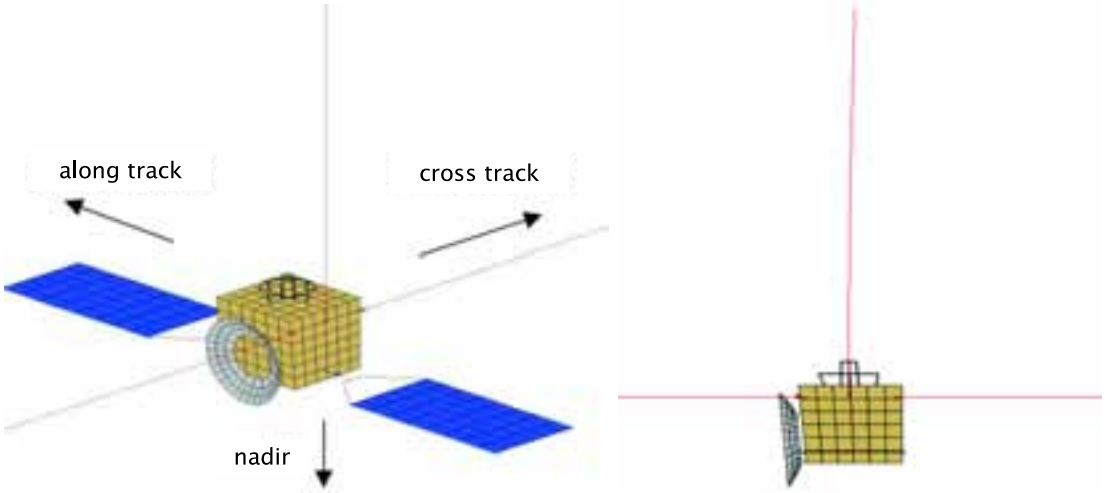

Figure 1: Mars Express wire-grid model (central body $\approx 1.6 \times 1.7 \times 1.4\,m$). The two dipole arms (20 m each) lie horizontal in the right-hand figure, and the monopole (7 m) is vertical. The antennas are cut as they jut out of the figure. The right-hand figure shows a slightly bent monopole. This configuration is used to investigate the influence of an eventual bend due to thermal heating.

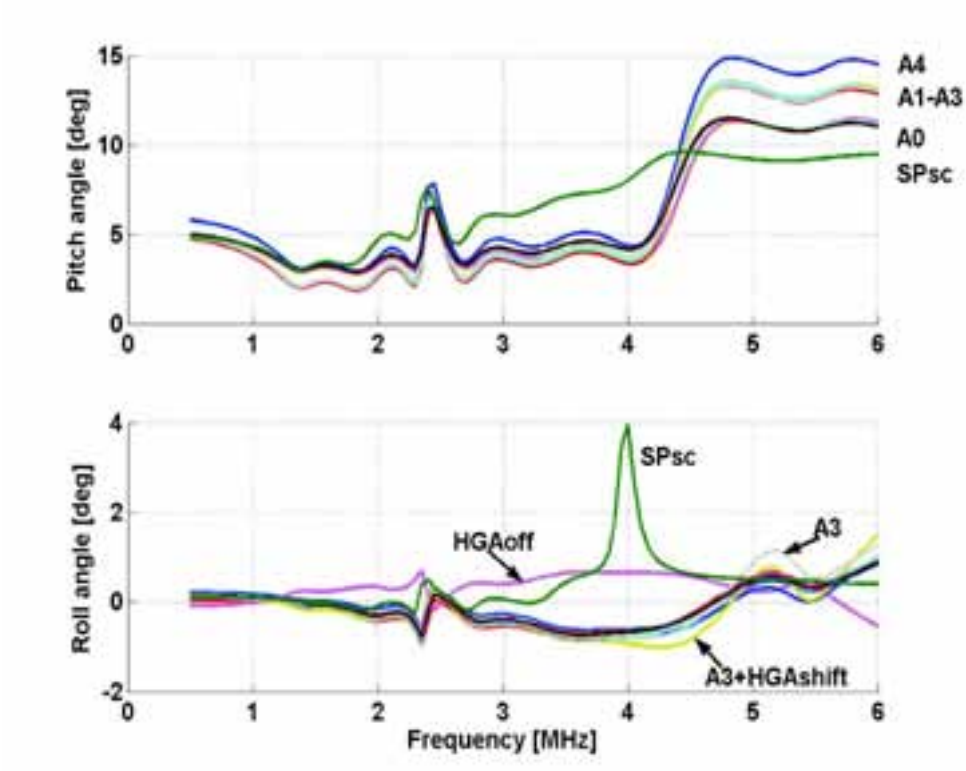

Figure 2: Monopole null-axis as a function of frequency for various spacecraft and feed configurations (explanation of curve annotation in text). Pitch and roll angles are rotation angles around cross-track and along-track directions, respectively.

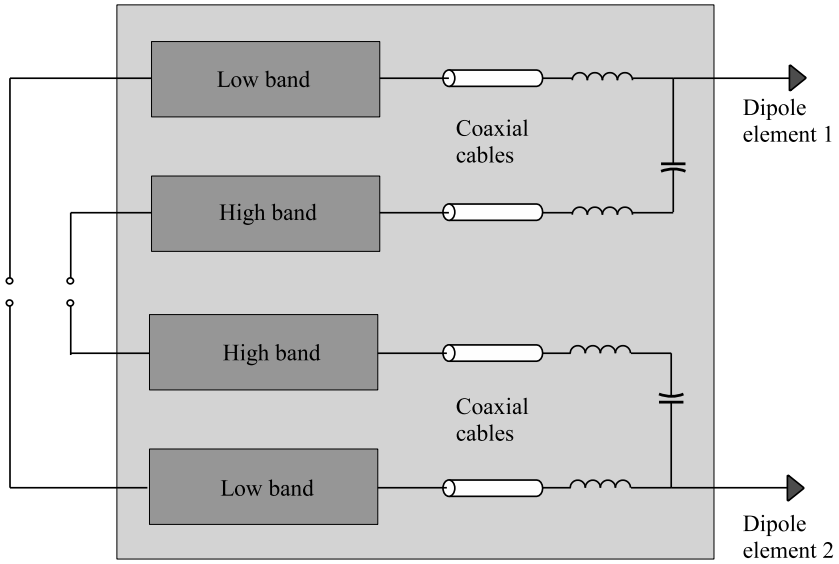

Figure 3: Block diagram of dipole matching network. Each dipole arm is connected to a separate network. The two networks are equivalent, each consisting of two sub-networks (filters), one dedicated to the low-frequency band (1.3–2.3) MHz, and the other dedicated to the three high frequency bands (2.5–5.5) MHz. The passive elements (like the coaxial cables) between antennas and filters are included in the network representation.

Each network consists of two sub-networks, a low-band and a high-band filter. Actually, the radar works with 4 different radar bands for subsurface sounding operation:

$$(1.3\text{–}2.3)\,\text{MHz},\quad (2.5\text{–}3.5)\,\text{MHz},\quad (3.5\text{–}4.5)\,\text{MHz},\quad (4.5\text{–}5.5)\,\text{MHz}.$$

The first radar band (1.3–2.3) MHz uses the two low-band filters, and the 3 other bands (2.5–5.5) MHz use the two high-band filters.

During the transmission phase a power amplifier is providing a high modulated voltage, which is applied to the respective network input. During the reception phase the voltages induced by the radio echoes at the dipole feeds are transmitted back to the receiver through the matching network. The case of the monopole antenna is different: there is no matching network but a preamplifier, which is represented as a very high impedance according to its input impedance. Cables and mountings capacitances are taken into account as base admittances between the respective antenna terminals.

3 Monopole gain and null axis

As the monopole is anti-nadir directed, its gain has a dedicated minimum near nadir. But the minimum is not exactly at nadir owing to the radiation coupling between the monopole and the parasitic bodies (spacecraft, dipole, solar panels, ...). This can be seen from the top panel of Figure 4, which depicts the monopole gain for the hemisphere turned towards Mars. The direction of the monopole null axis (direction of minimum gain) is slightly tilted along track from nadir. With increasing frequency the pattern

distorts more and more, and the minimum flattens out, getting elongated in cross-track direction.

Different model geometries are investigated to explore the influence of the spacecraft and feed configurations on the direction of the monopole null axis (Figure 2). The orientation of the null axis is defined by pitch angle (rotation around cross-track axis, parallel to dipole arms) and roll angle (rotation around along-track axis, parallel to solar panels). The annotation of the curves indicates the following configurations: A0–A4 belong to different antenna feed positions, A4 (blue) being the most realistic configuration; SPsc signifies that the Solar Panels are short-circuited to the s/c, all other configurations use 2 kΩ resistors between the Solar Panels and the s/c which is the real case (for ESD control, limiting the current in case of a fault in the solar cell array wiring shorting to the solar array chassis); HGAoff marks the profile obtained if the High Gain Antenna (HGA) were taken off. The antenna configurations A0-A4 differ in the position of the feeds, namely the distances from the near edge of the main body (variations by 10–20 cm). The results show that the pitch angle of the null axis is very sensitive to these variations, whereas the roll angle is rather unmoved. The virtual spacecraft without HGA behaves quite different as could be expected. The curve marked HGAshift is calculated with the HGA offset 20 cm parallel to the nearest main body surface. It shows that the results are quite stable with regard to the precision of the HGA mounting position. A very important effect is due to the resistances inserted between the solar panels and the main body. The profile for short-circuited resistances deviates considerably from the others, having a roll angle peak at about 4 MHz. This emphasizes the importance of these resistors.

4 Monopole compound gain

The monopole gain patterns do not take into account the polarization of the waves, which is essential in the calculation of the signal finally received from the echoes returning to the spacecraft. In order to express how the polarization properties of the antennas affect the received voltages, the compound gain

$$G^{\mathrm{c}} \sim \left| \frac{V^{\mathrm{r}}}{V^{\mathrm{t}}} \right|^2 \tag{1}$$

is introduced, where V^{t} is the voltage at the dipole matching network input when transmitting, and V^{r} is the corresponding voltage for the monopole or dipole, respectively, when receiving. G^{c} represents the received power of monopole or dipole, respectively, per unit power delivered at transmission. This takes into account the quality of polarization matching between the transmitting and receiving antenna and the distance from the surface. Our calculations assume that the surface reflects the waves completely and that the polarization state is unchanged as well. Taking into account the roughness and dielectric properties of the surface would allow us to better model the polarization of the reflected echoes but is beyond the scope of this article.

The middle panel of Figure 4 illustrates the monopole compound gain $G^{\mathrm{c}}_{\mathrm{mon}}$ with the s/c being 800 km above the surface. A comparison with the monopole gain G_{mon} (top

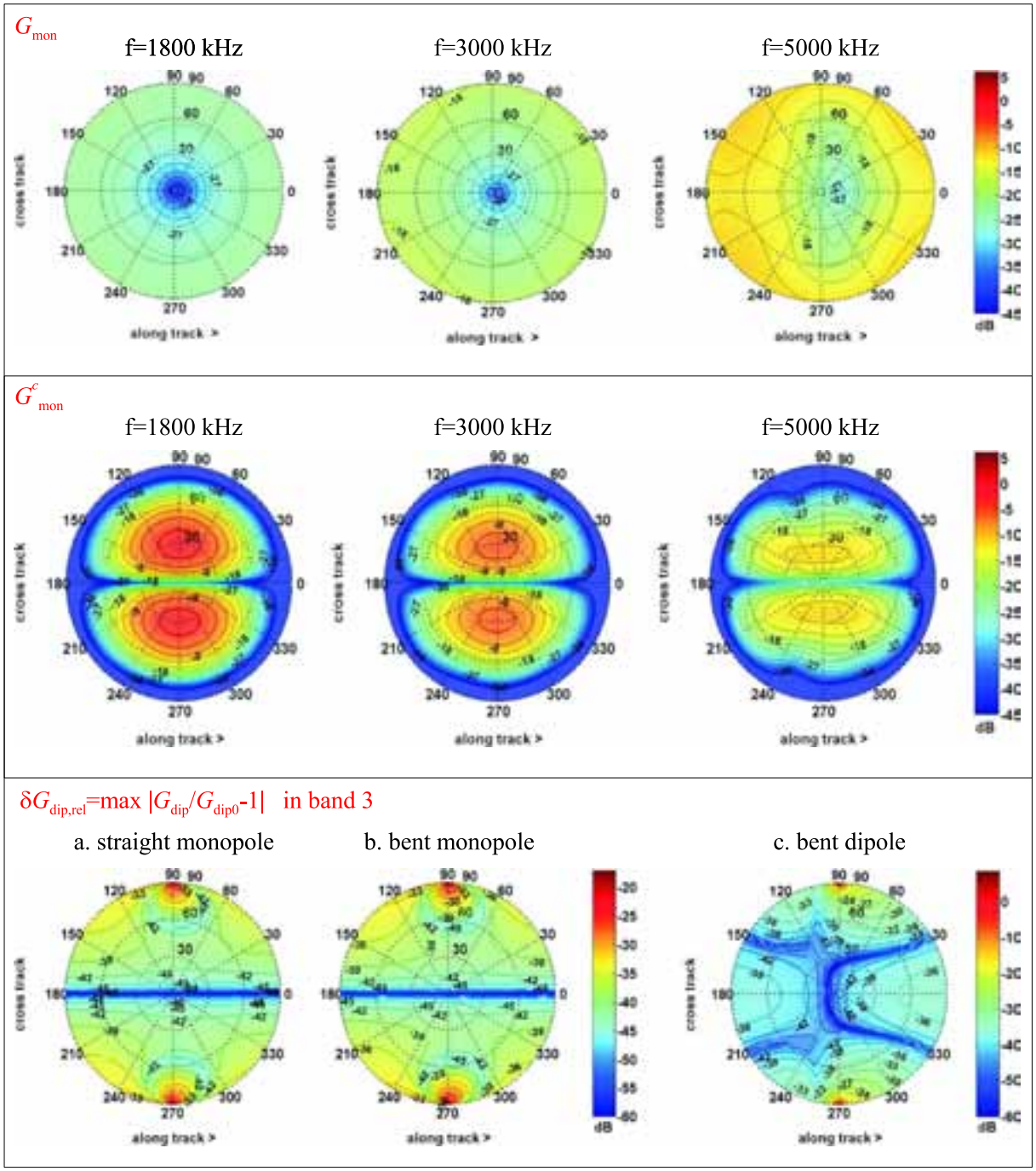

Figure 4: Polar diagrams representing gain patterns for the hemisphere facing Mars as seen from the spacecraft. Top: Monopole gain for 3 frequencies. Middle: Normalized monopole compound gain for 3 frequencies. Bottom: Maximum relative error (in dB) of dipole gain in band 3 (3.5–4.5 MHz) due to these configuration changes: a. deployment of the straight monopole; b. deployment of the monopole bent by 10 cm cross-track tip offset; c. bending of the dipole (20 cm tip offset) with the monopole being unchanged (deployed).

panel of Figure 4) reveals that the patterns are completely different. Two aspects can be recognized clearly: First, $G^{\mathrm{c}}_{\mathrm{mon}}$ vanishes when approaching the horizon because of the increasing distance to the Martian surface. Second, $G^{\mathrm{c}}_{\mathrm{mon}}$ does not have a pronounced minimum near nadir like G_{mon}. Instead, there is an along track valley crossing nadir. The pattern is almost symmetric with regard to the along track-nadir plane. As a consequence the monopole does not see echoes returning from this valley, in particular it is blind to echoes from nadir. But the monopole is sensitive to cross-track clutters, having the same sensitivity for positive and negative cross-track (roll) angles. All these facts prove that the monopole-dipole configuration is suitable for the cross-track clutter cancellation. The precondition of this assessment is that the radar waves do not experience significant depolarization at surface reflection. In this case of polarization conservation the slight offset of the monopole null-axis from nadir does not matter so much for the cross-track clutter cancellation.

5 Influence of the monopole on the dipole

A very important issue is the influence of the monopole on the reception properties of the dipole. Since the monopole is mainly used for clutter cancellation and the dipole provides the primary signal which is to be Doppler azimuth processed, it is desirable that this influence remains very small over all 4 frequency bands from 1.3 to 5.5 MHz. Therefore we compared the nominal situation where all antenna elements are deployed with the option of a non-deployed monopole (Figure 4a, bottom panel). The quantity used in order to get an impression of how various effects interfere with the nominal properties of the dipole, is the relative error of the dipole gain in dB, i.e.

$$\delta G_{\mathrm{dip,rel}} = \max_{f \in \mathrm{band}} \left| \frac{G_{\mathrm{dip}} - G_{\mathrm{dip0}}}{G_{\mathrm{dip0}}} \right|, \tag{2}$$

where G_{dip0} denotes the nominal value of the gain (without interference). The resulting relative error in dipole gain is below –40 dB within 30 degrees around nadir. This estimation also holds when the deployed monopole is bent — possibly due to imprecise deployment or solar heating (Figure 4b). The influence of dipole bent due to solar heating on the dipole gain is even much smaller (Figure 4c). In consequence, the influence of the monopole deployment and of an eventual dipole bent due to solar heating on the dipole properties are practically negligible.

6 Conclusion

The calculations of the transmission and reception properties of the antennas of the Mars Express/MARSIS radar experiment show that

- there is a strong dependence of the monopole null-axis on frequency and on certain configuration details, mostly dominated by the solar panels, the high gain antenna and the asymmetric mounting of the antennas,

- the polarization of the transmitted radar pulses is not matched to the monopole (mostly linear polarization close to nadir with the electric field being nearly orthogonal to the monopole), so no clear minimum of the compound gain pattern is present, but an along-track valley in the polar plots appears,
- as a result the monopole voltage received from the echoes is much more cross-track sensitive than along-track sensitive, which is beneficial to clutter cancellation,
- the influence of the monopole deployment on the dipole gain is highest in band 4, but negligibly small, i.e. below –40 dB relative change within 30 degrees from nadir,
- bending of dipole and monopole due to solar heating does not change the dipole reception properties appreciably. However, monopole bend may slightly change the monopole null-axis.

In summary, the monopole-dipole antenna system is well configured for the cross-track clutter cancellation for radar waves that do not experience significant depolarization at surface reflection. The monopole does not disturb the dipole reception properties and the effect of an eventual bending of the antennas due to solar heating is practically negligible. But one has to take account of the deviation of the real dipole pattern from that of an ideal dipole and the frequency dependence of the antenna properties, which may affect the signal processing.

Acknowledgements

We appreciate the provision of information on the MARSIS instrument by the MARSIS team. We especially thank G. Picardi, A. Masdea and A. Safaeinili for valuable discussions on the radar technique, and D. Kirchner and R. Huff for information on the matching network.

References

Harrington, R.F., *Field Computation by Moment Methods*, R.E. Krieger Publishing Company, Malabar, Florida, 1968.

Macher, W., B. Schraußer, G. Fischer, H.O. Rucker, H. Lammer, C. Kolb, and G. Kargl, Analysis of Sounding Antennas of the Mars Express MARSIS Experiment, Proc. 2nd European Workshop on Exo/Astrobiology, Graz, SP-518, 539, 2002.

Picardi, G., S. Sorge, R. Seu, G. Fedele, C. Federico, R. Orosei, Mars Advanced Radar for Subsurface and Ionosphere Sounding (MARSIS): models and system analysis. Infocom Technical Report Nr. 007/005/99, 1999.

Picardi, G., D. Biccari, R. Seu, L. Marinangeli, W.T.K. Johnson, R.L. Jordan, J. Plaut, A. Safaeinili, D.A. Gurnett, G.G. Ori, R. Orosei, D. Calabrese, E. Zampolini, Performance and surface scattering models for the Mars Advanced Radar for Subsurface and Ionosphere Sounding (MARSIS), *Planet. Space Sci.*, **52**, 149—156, 2004.